International Journal of Engineering and Advanced Technology (IJEAT)
ISSN: 2249 – 8958, Volume-8 Issue-6S2, August 2019

Analysis of the Small Signal Stability of the Power System Connected with Wind Generators

Anithasampathkumar, Aarthi Suriya, S.Sherine

Abstract*: *The fundamental goal of this proposal is to contemplate and examine the little signal soundness of the power framework associated with wind generators, as the power age utilizing wind generators has picked up significance in the ongoing days.

Here, direct drive perpetual magnet synchronous generator is considered in the investigation, and the little sign model is inferred to survey the little unsettling influence solidness. The eigen esteem examination explores the dynamic conduct of intensity framework under various modes. Along these lines, by utilizing eigen esteem investigation, the connection between the modes and the state factors are gotten. In this manner by fluctuating the controller parameters their effect on the eigen esteems are considered. The outcome demonstrates that the framework soundness can be improved by appropriate tuning of both generator side and matrix side converter controller parameters. [1],[3],[5]

Little sign model is produced for a matrix associated PMSG based WECS. Eigen esteem examination is performed for 3 machine nine 9 transport framework utilizing MATLAB/SIMULINK.

Keywords:MATLAB,power,generator

I. INTRODUCTION

The accessibility of electrical vitality is a need for the working of present day social orders. The vitality utilization is expanding tremendously as of late, because of enormous industrialization. The dangers of lack of fossil issues and their consequences for the climatic change accentuation the utilization of exchange asset (sustainable power source). The principle points of interest of power age from sustainable sources are the nonattendance of unsafe discharges and interminable accessibility of the crude material for transformation. [2],[4],[6]

The different accessible inexhaustible assets are sun powered, hydro, wind and so on. The age of electrical power from wind homesteads is growing quickly with overall introduced limit. As of now India stands fifth in the generation of power from wind cultivates after China, USA, Germany, and Spain. The introduced limit in India is 16,000 MW.

In addition, of its bit of leeway wind vitality age additionally has its weaknesses, for example, multifaceted nature, cost, and flimsiness of wind speed. The cost detriment is decreased by endowments from Government as they are probably going to advance the green power age. Then again, cost of wind power is moderately lower when contrasted with other sustainable power source assets.

The conduct of intensity framework is for the most part dictated by the conduct and collaboration of generators associated with it. At the point when the infiltration of wind age builds its impact on power framework likewise increments. This prompts cautious investigation of dependability of intensity framework with wind generators. In this proposition, the impact of matrix associated variable speed wind vitality change framework on the solidness of intensity framework is contemplated. [7],[9] ,[11]

II. MODELLING OF POWER SYSTEM COMPONENTS FOR STABILITY ANALYSIS

Dynamic model of matrix associated wind vitality transformation framework is required to accomplish learning about progressing change in the framework because of expanding wind vitality entrance. This part manages the numerical demonstrating of intensity framework comprising of differential and logarithmic conditions speaking to the models of framework segments including synchronous generators, loads. [8],[10] ,[12]

A. WIND TURBINE MODEL

The power extracted from the wind is given by,

$$T_m = \frac{\rho A V^3 C_p}{2\omega_r S_b} \quad 2.1$$

$$\lambda = \frac{\omega_r R}{V} \quad (2.2)$$

Revised Manuscript Received on August 22, 2019.

Anitha Sampathkumar, Department of EEE,Bharath Institute of Higher Education and Research, Tamilnadu, India. Email: anithababs@gmail.com

S.Aarthi Suriya, Department of EEE,Bharath Institute of Higher Education and Research, Tamilnadu, India. Email: aarthisuriya2703@gmail.com

S.Sherine, Department of EEE,Bharath Institute of Higher Education and Research, Tamilnadu, India. Email: nssherine@gmail.com

A general functional representation of C_P is given by Lubosny (2003) as,

$$C_p = C_1(C_2 h - C_3\beta - C_4)e^{-C_5 h} \qquad (2.3)$$

Where,

$$h = \frac{1}{\lambda + 0.08\beta} - \frac{0.035}{\beta^3 + 1} \qquad (2.4)$$

C_1 to C_6 are constants. The C_P versus λ curve is provided by the manufacturer. The constants C_1 to C_6 are computed for particular turbines using the procedure given by Heier (1998).

B.MODEL OF SYNCHRONOUS GENERATORS

.

The differential equations of synchronous generators

$$\frac{d\delta_i}{dt} = \omega_i - \omega_s \qquad (2.5)$$

$$\frac{2H_i}{\omega_s}\frac{d\omega_i}{dt} = T_{Mi} - T_{ei} - D_i(\omega_i - \omega_s) \qquad (2.6)$$

$$T_{doi}\frac{dE'_{qi}}{dt} = -E'_{qi} - (X_{di} - X'_{di})I_{di} + E_{fdi} \qquad (2.7)$$

$$T'_{qoi}\frac{dE_{di}}{dt} = -E'_{di} + (X_{qi} - X'_{qi})I_{qi} \qquad (2.8)$$

$$T_{ei} = E'_{di} I_{di} + E'_{qi} I_{qi} + (X'_{qi} - X'_{di}) \qquad (2.9)$$

The stator algebraic equations are represented as follows

$$E'_{di} - V_i \sin(\delta_i - \theta_i) - R_{si} I_{di} + X'_{qi} I_{qi} = 0$$
$$E'_{qi} - V_i \cos(\delta_i - \theta_i) - R_{si} I_{qi} - X'_{di} I_{di} = 0$$

C.MODEL OF INDUCTION GENERATOR

The enlistment generator is spoken to by methods for surely understood third request model. The stator homeless people are ignored, and adjusted activity of the enlistment generator is expected. The enlistment machine model includes two rotor windings on the d and q tomahawks. This, thus, suggests two state factors on the tomahawks that characterize the electric drifters of the rotor. Utilizing again generator flow show, the electric torque of the acceptance machine is

$$T_{ei} = E'_{di} I_{di} + E'_{qi} I_{qi} \qquad (2.12)$$

The dynamic response of the electrical states is described by the differential equations

$$\frac{dE'_r}{dt} = -\frac{[E'_r + (Xo - X')I_m]}{T'_o} - s\omega_s E'_m$$

(2.13)

$$\frac{dE'_m}{dt} = -\frac{[E'_m - (Xo - X')I_r]}{T'_o} + s\omega_s E'_r$$

(2.14)

$$E'_{ri} - V_i \cos(\theta_i) - RI_{di} + X'_{si} I_{mi} = 0$$
$$E'_{mi} - V_i \sin(\theta_i) - R_{si} I_{mi} - X'_{si} I_{ri} = 0$$

(2.15)

A squirrel-confine enlistment machine associated with an AC power wellspring of fitting voltage can work either as an engine or as a generator. The terminal voltage applied to the machine produces slacking charging current, which thus brings about the pivoting attractive field inside the air hole for both motoring and creating activity. At the point when the engine is stacked, current streams in shortcircuited rotor because of the rotor EMF and the engine keeps running at sub-synchronous speed. [13], [15] ,[17]

At the point when the acceptance machine keeps running at super-synchronous speed, a voltage is incited in the rotor in stage resistance to the EMF instigated as a result of inversion of relative speed. The part of the stator current, which adjusts the rotor MMF, likewise turns around. The stator current presently comprises of polarizing present as in the past and a segment in stage restriction to the stator applied voltage. In this manner the machine turns into an acceptance generator with outside excitation. The acceptance generator can be spoken to by the notableproportional circuit appeared in Fig

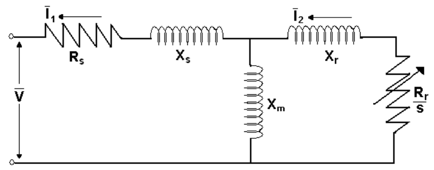

Fig 2.1 Steady state equivalent circuit of induction generator

From Fig2.1, the current I_1 can be written as,

$$\bar{I}_1 = \frac{\bar{V}}{(R_s + R_e) + j(X_s + X_e)}$$

(2.16)

Where,

$$R_e + jX_e = \frac{jX_m\left(\frac{R_r}{s} + jX_r\right)}{\frac{R_r}{s} + j(X_m + X_r)}$$

(2.17)

$$P_g = I_2^2 \frac{R_r}{s} \quad (2.18)$$

The electrical power developed in the rotor is,

$$P_e = I_2^2 \frac{R_r}{s}(1-s)$$

(2.19)

Where the slip is negative. The electrical torque developed is then given by,

$$\tau_e(V,s) = \frac{V^2 X_m^2 \frac{R_r}{s}}{\left[\left(R_x + \frac{R_r}{s}\right)^2 + (X_x + X_r)^2\right]\left[R_s^2 + (X_s + X_m)^2\right]}$$

(2.20)

Where,

$$R_x + jX_x = \frac{jX_m(R_s + jX_r)}{R_s + j(X_s + X_m)}$$

(2.21)

MODEL OF PMSG

Using Source convention, voltage equations of PMSG in d-q reference frame (q-axis leads d-axis in the direction of rotation) is

$$V_{ds}^{\varphi} + R_s i_{ds}^{\varphi} + \omega \psi_{qs}^{\varphi} = 0 \quad (2.22)$$

$$V_{qs}^{\varphi} + R_s i_{qs}^{\varphi} + \omega \psi_{ds}^{\varphi} = 0 \quad (2.23)$$

The flux linkage equations of PMSG is

$$\psi_{qs}^{\varphi} = -L_q i_{qs}^{\varphi} \quad (2.24)$$

$$\psi_{ds}^{\varphi} = \psi_f \quad (2.25)$$

The active and reactive power equations are given by

$$P_s = V_{ds}^{\varphi} i_{ds}^{\varphi} + V_{qs}^{\varphi} i_{qs}^{\varphi} \quad (2.26)$$

$$Q_s = V_{ds}^{\varphi} i_{qs}^{\varphi} - V_{qs}^{\varphi} i_{ds}^{\varphi} \quad (2.27)$$

MODEL OF DRIVE TRAIN

The rotor of wind turbine and generator are connected directly, so they can be expressed together by

$$\dot{\omega}_r = \frac{1}{H}(T_m - T_e)$$

(2.28)

$$\dot{\delta} = \omega_s(\omega_r - 1)$$

(2.29)

Where

H- Equivalent inertia time constant of whole drive train.

T_m - mechanical torque.

T_e - Electro-magnetic torque.

MODEL OF CONVERTERS AND THEIR CONTROLLERS

$$i_{ds}^{\varphi} = 0$$

(2.30)

$$i_{qs}^{\varphi} = \frac{k_{pw}}{\psi_s}(\omega_{rref} - \omega_r) + X_w$$

(2.31)

$$\dot{X}_w = \frac{k_{pw}}{T_w}(\omega_{rref} - \omega_r)$$

(2.32)

EQUATIONS OF GRID SIDE CONTROLLER

When the direction of q-axis is aligned with the voltage vector

, then V_{dg} =0.

$$P_g = V_{qg}^{\varepsilon} i_{qg}^{\varepsilon}$$

(2.33)

$$Q_g = V_{qg}^{\varepsilon} i_{dg}^{\varepsilon}$$

(2.34)

Here d-Axis grid side current i_{dg} is controlled to maintain terminal voltage and q-Axis grid side current i_{qg} is controlled to obtain constant dc link voltage.

$$i_{dg}^{\varepsilon} = k_{pv}(V_{dcref} - V_{dc}) + X_v$$

(2.35)

$$i_{qg}^{\varepsilon} = k_{p1}(V_{tref} - V_t) + X_4$$

(2.36)

$$\dot{X}_v = \frac{k_{pv}}{T_v}(V_{dcref} - V_{dc})$$

(2.37)

$$\dot{X}_4 = \frac{k_{p1}}{T_4}(V_{tref} - V_t)$$

(2.38)

EQUATION OF DC LINK VOLTAGE

The equation of dc link part is given by

$$\dot{V}_{dc} = \frac{1}{CV_{dc}}(V_{qs}^{\varphi} i_{qs}^{\varphi} - V_{da}^{\varepsilon} i_{dg}^{\varepsilon})$$

(2.39)

Where, C - Dc link capacitor.

D.INTERFACING WITH POWER SYSTEM

PMSG connected to 3 rd bus of 3 machine nine bus system through a transmission line and transformer. The voltage equation describing the interface with the external system can be written as

$$V_{da} = V_{dg} - L i_{qg}$$

(2.40)

$$V_{qa} = V_{qg} + L i_{dg}$$

(2.41)

Where, L is sum of transmission line and transformer inductance.

E.NETWORK MODEL

The system can be demonstrated in power equalization or current parity structure. In this theory, control equalization type of system portrayal is embraced. As announced by Peter W.Sauer and M.A. Pai (2002), the power equalization structure has some additional highlights than the present parity structure. In this structure, the all-inclusive DAE framework Jacobian contains data about burden stream Jacobian. The various kinds of burdens can be effectively consolidated in this model. The network equations for generator buses are: [14],[16], [18]

$$I_{di}V_i \sin(\delta_i - \theta_i) + I_{qi}V_i \cos(\delta_i - \theta_i) + P_{Li} - \sum_{k=1}^{n} V_i V_k Y_{ik} \cos(\theta_i - \theta_k - \alpha_{ik}) = 0$$

(2.42)

$$I_{di}V_i \cos(\delta_i - \theta_i) - I_{qi}V_i \sin(\delta_i - \theta_i) + Q_{Li} - \sum_{k=1}^{n} V_i V_k Y_{ik} \sin(\theta_i - \theta_k - \alpha_{ik}) = 0$$

(2.43)

Where i= 1: m no of machines.

The network equations for load buses are:

$$P_{Li} - \sum_{k=1}^{n} V_i V_k Y_{ik} \cos(\theta_i - \theta_k - \alpha_{ik}) = 0$$

(2.44)

$$Q_{Li} - \sum_{k=1}^{n} V_i V_k Y_{ik} \sin(\theta_i - \theta_k - \alpha_{ik}) = 0$$

(2.45)

Where i= m+1 to n no of buses.

III.SMALL SIGNAL MODEL OF POWER SYSTEM COMPONENTS

In this approach, the network equations are written in power balance form. Although equivalent to the current balance form, it has some extra features. The extended DAE system Jacobian also contains information about the load flow Jacobian. [19],[20],[21]

SMALL SIGNAL MODEL FOR SYNCHRONOUS GENERATORS

$$\overset{\bullet}{\Delta x} = A_1 \Delta x + A_2 \Delta I_g + A_3 \Delta \hat{V}_g + E \Delta U$$

(3.1)

Where A_1=Diag(A_{1i}), A_2=Diag(A_{2i}), A_3=Diag(A_{3i}) and E=Diag(E_i)

$$A_{1i} = \begin{bmatrix} -\frac{D_i}{M_i} & 0 & -\frac{I_{qi0}}{M_i} & -\frac{I_{di0}}{M_i} & 0 \\ \omega_s & 0 & 0 & 0 & 0 \\ 0 & 0 & -\frac{1}{T'_{d0i}} & 0 & \frac{1}{T'_{d0i}} \\ 0 & 0 & 0 & -\frac{1}{T'_{q0i}} & 0 \\ 0 & 0 & 0 & 0 & \frac{-1}{T_A} \end{bmatrix}$$

$$A_{2i} = \begin{bmatrix} -\frac{[(X'_d - X'_q)I_{d0} + E'_{q0}]}{M_i} & -\frac{[(X'_d - X'_q)I_{q0} + E'_{d0}]}{M_i} \\ 0 & 0 \\ 0 & \frac{(X_d - X'_d)}{T'_{d0}} \\ -\frac{(X_q - X'_q)}{T'_{q0}} & 0 \\ 0 & 0 \end{bmatrix}$$

$$A_{3i} = \begin{bmatrix} 0 & 0 \\ 0 & 0 \\ 0 & 0 \\ 0 & 0 \\ 0 & \frac{1}{T_A} \end{bmatrix}$$

$$0 = B_1 \Delta x + B_2 \Delta I_g + B_3 \Delta \hat{V}_g$$

The stator algebraic equations (2.10) are linearized as (3.2)

Where

$$\Delta x^T_i = [\Delta\omega_i \quad \Delta\delta_i \quad \Delta E'_{qi} \quad \Delta E'_{di} \quad \Delta E_{fdi}]$$

$$\Delta I^T_{gi} = [\Delta I_{qi} \quad \Delta I_{di}]$$

$$\Delta \hat{V}_{gi}^{T} = [\Delta\theta_{gi} \quad \Delta V_{gi}]$$

$$\Delta \hat{V}_{li}^{T} = [\Delta\theta_{li} \quad \Delta V_{li}]$$

Where B_1=Diag(B_{1i}), B_2=Diag(B_{2i}), B_3=Diag(B_{3i})

$$B_{1i} = \begin{bmatrix} 0 & V_{i0}\sin(\delta_{i0} - \theta_{i0}) & 1 & 0 & 0 \\ 0 & -V_{i0}\cos(\delta_{i0} - \theta_{i0}) & 0 & 1 & 0 \end{bmatrix}$$

$$B_{2i} = \begin{bmatrix} R_{si} & -X'_{qi} \\ X'_{di} & R_{si} \end{bmatrix}$$

$$B_{3i} = \begin{bmatrix} -V_{i0}\cos(\delta_{i0} - \theta_{i0}) & \sin(\delta_{i0} - \theta_{i0}) \\ V_{i0}\sin(\delta_{i0} - \theta_{i0}) & \cos(\delta_{i0} - \theta_{i0}) \end{bmatrix}$$

The network equations (2.42) and (2.45) are linearized to obtain

Retrieval Number: F10030886S219/2019©BEIESP
DOI:10.35940/ijeat.F1003.0886S219

Published By:
Blue Eyes Intelligence Engineering
& Sciences Publication

$$0 = C_1\Delta x + C_2\Delta I_g + C_3\Delta\hat{V}_g + C_4\Delta\hat{V}_l$$

$$0 = C_1\Delta x + C_2\Delta I_g + C_3\Delta\hat{V}_g + C_4\Delta\hat{V}_l$$

(3.3)

C_1 and C_2 are block diagonal matrices and C_3, C_4, D_1, and D_2 are full matrices .The block diagonal matrices are

$$C_{1i} = \begin{bmatrix} 0 & I_{di0}V_{i0}\cos(\delta_{i0}-\theta_{i0}) & 0 & 0 & 0 \\ 0 & -V_{i0}I_{qi0}\sin(\delta_{i0}-\theta_{i0}) & 0 & 0 & 0 \end{bmatrix}$$

$$C_{2i} = \begin{bmatrix} V_{i0}\sin(\delta_{i0}-\theta_{i0}) & V_{i0}\cos(\delta_{i0}-\theta_{i0}) \\ V_{i0}\cos(\delta_{i0}-\theta_{i0}) & -V_{i0}\sin(\delta_{i0}-\theta_{i0}) \end{bmatrix}$$

$$\Delta I_g = -B^{-1}{}_2 B_1\Delta x - B^{-1}{}_2 B_3\Delta\hat{V}_g \qquad (3.4)$$

Since ΔI_g is not of interest, it can be eliminated from using (3.2) and (3.3). Using ΔI_g from (3.2) as,

$$\dot{\Delta x} = (A_1 - A_2B^{-1}{}_2B_1)\Delta x - (A_3 - A_2B^{-1}{}_2B_3)\Delta\hat{V}_g + E\Delta u$$

$$0 = (C_1 - C_2B^{-1}{}_2B_1)\Delta x - (C_3 - C_2B^{-1}{}_2B_3)\Delta\hat{V}_g + C_4\Delta\hat{V}_l + \Delta S_{LG}(V)$$

$$0 = D_1\Delta\hat{V}_g + D_2\Delta\hat{V}_l + \Delta S_{Ll}(V)$$

$$\dot{\Delta x} = A'_1\Delta x + A'_3\Delta\hat{V}_g + E\Delta u$$

$$0 = C'_1\Delta x + C'_3\Delta\hat{V}_g + C'_4\Delta\hat{V}_l$$

$$0 = D'_1\Delta\hat{V}_g + D'_4\Delta\hat{V}_l$$

$$\dot{\Delta x} = A_{sys}\Delta x + E\Delta u$$

$$A_{sys} = A'_1 - [A'_2\ A'_3]^{-1}\begin{bmatrix} B_1 \\ C_1 \end{bmatrix}$$

$$\begin{bmatrix} \dot{\Delta x}_{sgi} \\ 0 \\ 0 \\ 0 \end{bmatrix} = \begin{bmatrix} A_{SGi} & 0 & A_2 & A_3 & A_4 \\ B_1 & & B_2 & B_3 & B_4 \\ C_1 & & C_2 & C_3 & \\ D_1 & & D_2 & & D_4 \end{bmatrix}\begin{bmatrix} \Delta x_{sgi} \\ \Delta xI_{d-q} \\ \Delta\hat{V}_{gi} \\ \Delta\hat{v}_l \end{bmatrix}$$

Linearising the differential Equations (2.12) to (2.14),

(3.7)

INCLUSION OF INDUCTION

$$\frac{d\Delta E'_r}{dt} = -\frac{[\Delta E'_r - (Xo - X')\Delta I_m]}{T'_o} + s_0\omega_s\Delta E'_m + \Delta\omega_r\omega_s E'_{m0}$$

$$\frac{d\Delta E'_m}{dt} = -\frac{[\Delta E'_m + (Xo - X')\Delta I_r]}{T'_o} - s_0\omega_s\Delta E'_r - \Delta\omega_r\omega_s E'_{r0}$$

$$\frac{d\Delta\omega}{dt} = \frac{\Delta T_m}{2H} - \frac{\Delta T_e}{2H}$$

(3.8)

Linearising the stator algebraic Equations (2.15)

$$\Delta E'_r + X'_s\,\Delta I_m - R_1\Delta I_r + V_{i0}\sin\theta_{i0}\Delta\theta_i - \cos\theta_i\Delta V_i = 0$$

$$\Delta E'_m - X'_s\,\Delta I_r - R_1\Delta I_m - V_{i0}\cos\theta_{i0}\Delta\theta_i - \sin\theta_i\Delta V_i = 0$$

(3.9)

The linearized state model Δx_{IG} added to the state space model $[\Delta\omega_r\ \Delta E'_r\ \Delta E'_m]$ b

(3.10)

And the

$$\begin{bmatrix} \dot{\Delta x}_{sgi} \\ \dot{\Delta x}_{igi} \\ 0 \\ 0 \\ 0 \end{bmatrix} = \begin{bmatrix} A_{SGi} & 0 & A_2 & A_3 & A_4 \\ 0 & A_{IG} & & & \\ B_1 & & B_2 & B_3 & B_4 \\ C_1 & & C_2 & C_3 & \\ D_1 & & D_2 & & D_4 \end{bmatrix}\begin{bmatrix} \Delta x_{sgi} \\ \Delta x_{igi} \\ \Delta xI_{d-q} \\ \Delta\hat{V}_{gi} \\ \Delta\hat{v}_l \end{bmatrix}$$

(3.11)

Linearising the differential Equations (2.1) to (2.4) and (2.22) to (2.41),

The differential equations after linearisation

$$\frac{d\Delta\omega}{dt} = \frac{\Delta T_m}{2H} - \frac{\Delta T_e}{2H}$$

(3.12)

$$\frac{d\Delta\delta}{dt} = \omega_s\Delta\omega$$

(3.13)

$$\frac{d\Delta V_{dc}}{dt} = \frac{1}{CV_{dc0}}(V^{\varphi}_{qs0}i^{\varphi}_{qs0} - V^{\varepsilon}_{da0}i^{\varepsilon}_{dg0}) - \frac{\Delta V_{dc}}{CV^2_{dc0}}(V^{\varphi}_{qs0}\Delta i^{\varphi}_{qs} - V^{\varepsilon}_{da0}\Delta i^{\varepsilon}_{dg} + $$

(3.14)

$$\frac{d\Delta X_w}{dt} = \frac{K_{pw}}{T_w}(-\Delta\omega)$$

(3.15)

$$\frac{d\Delta X_v}{dt} = \frac{K_{pv}}{T_v}(-\Delta V_{dc})$$

(3.16)

$$\frac{d\Delta X_4}{dt} = \frac{K_{p1}}{T_4}(-\Delta V)$$

(3.17)

The real and reactive power equations are given by

$$\Delta P_g = \Delta V_{da}^{\varepsilon} i_{dg0}^{\varepsilon} + \Delta i_{dg}^{\varepsilon} V_{da0}^{\varepsilon}$$

(3.18)

$$\Delta Q_g = -\Delta V_{da}^{\varepsilon} i_{qg0}^{\varepsilon} - \Delta i_{qg}^{\varepsilon} V_{da0}^{\varepsilon}$$

(3.19)

$$A_{PMSG} = \begin{bmatrix} \frac{K_{pw}+a_{11}}{2H} & 0 & 0 & a14 & 0 & 0 \\ \omega_s & 0 & 0 & 0 & 0 & 0 \\ a_{31} & 0 & a_{33} & a_{34} & a_{35} & a_{36} \\ a_{41} & 0 & 0 & 0 & 0 & 0 \\ 0 & 0 & a_{53} & 0 & 0 & 0 \\ 0 & 0 & 0 & 0 & 0 & 0 \end{bmatrix}$$

Where,

$$a_{11} = T_m \left[\left(\omega_{rpu} \times dC_p \times dh - d\lambda \right) - C_p \right]$$

(3.20)

$$a_{14} = \frac{-1}{2H}$$

(3.21)

$$a_{31} = \frac{-V_{qso}{}^{\varphi} K_{pw} + I_{qso}{}^{\varphi} R_s K_{pw}}{CV_{dco}\psi_s}$$

(3.22)

$$a_{33} = \frac{K_{pv} V_{dgo}{}^{\varepsilon}}{CV_{dco}} - \frac{V_{qso}{}^{\varphi} i_{qso}{}^{\varphi}}{CV_{dco}{}^2} + \frac{V_{dao}{}^{\varepsilon} i_{dgo}{}^{\varepsilon}}{CV_{dco}{}^2}$$

(3.23)

$$a_{34} = \frac{V_{qso}{}^{\varphi} - R_s i_{qso}{}^{\varphi}}{CV_{dc}\psi_s}$$

(3.24)

$$a_{35} = \frac{-V_{dgo}{}^{\varepsilon}}{CV_{dc}}$$

(3.25)

$$a_{36} = \frac{i_{dgo}{}^{\varepsilon} L}{CV_{dco}}$$

(3.26)

$$a_{41} = \frac{-K_{pw}}{T_w}$$

(3.27)

$$a_{53} = \frac{-K_{pv}}{T_v}$$

(3.28)

$$A_2 = \begin{bmatrix} 0 & 0 \\ 0 & 0 \\ 0 & a_{32} \\ 0 & 0 \\ 0 & 0 \\ 0 & a_{52} \end{bmatrix}$$

Where,

$$a_{32} = -\frac{i_{dg0}^{\varepsilon}}{CV_{dc0}}(1 + k_{p1}L)$$

(3.29)

$$a_{52} = \frac{-K_{p1}}{T4}$$

(3.30)

$$D_1 = \begin{bmatrix} 0 & 0 & -K_{pv}V_{dao}{}^{\varepsilon} & 0 & V_{dao}{}^{\varepsilon} & -Li_{dgo}{}^{\varepsilon} \\ 0 & 0 & 0 & 0 & 0 & d_{24} \end{bmatrix}$$

Where, $d_{24} = i_{qgo}{}^{\varepsilon} L - V_{dao}{}^{\varepsilon}$

(3.31)

$$D_4 = \begin{bmatrix} 0 & \left(K_{p1}L + 1\right) i_{dgo}{}^{\varepsilon} \\ 0 & d_{22} \end{bmatrix}$$

Where, $d_{22} = K_{p1}V_{dao}{}^{\varepsilon} - i_{qgo}{}^{\varepsilon} - K_{p1} i_{qgo}{}^{\varepsilon} L$

(3.32)

The linearized state model is added to the state space model by defining $\Delta X_{PMSG} = [\Delta\omega\ \Delta i_{dq}\ \Delta V_{dc}\ \Delta X_w\ \Delta X_v\ \Delta X_4]$

(3.33)

$$\begin{bmatrix} \dot{\Delta x}_{sgi} \\ \dot{\Delta x}_{igi} \\ \dot{\Delta x}_{PMSGi} \\ 0 \\ 0 \\ 0 \end{bmatrix} = \begin{bmatrix} A_{sgi} & 0 & 0 & A_2 & A_3 & A_4 \\ 0 & A_{igi} & 0 & & & \\ 0 & 0 & A_{PMSGi} & & & \\ B_1 & & & B_2 & B_3 & B_4 \\ C_1 & & & C_2 & C_3 & \\ D_1 & & & D_2 & & D_3 \end{bmatrix} \begin{bmatrix} \Delta X_{sgi} \\ \Delta X_{igi} \\ \Delta X_{PMSGi} \\ \Delta i_{d-q} \\ \Delta \hat{V}_{gi} \\ \Delta \hat{V}_l \end{bmatrix}$$

(3.34)

Because of the stochastic idea of wind speed, generator speed shifts constantly to follow the greatest power point. These speed varieties are converted into generator yield control varieties and thusly DC interface voltage changes. Subsequently, there emerges a requirement for composed tuning of MSC and GSC controllers. In any case, facilitated tuning of these controllers utilizing the customary experimentation technique is a lumbering and testing task. In this manner improvement strategies are being used for the planned tuning of controllers.

OPTIMISATION OF CONTROLLER PARAMETERS

IV.RESULTS AND DISCUSSION

This Chapter presents the small signal stability analysis 3 machine 9 bus system consisting of two synchronous generators and one PMSG based WECS. Then one induction generator is included in the system.

The system considered for analysis is shown in Appendix A.1. The data for this system is given in Appendix A. Here PMSG is connected to 3 rd bus and it is considered as load bus.The load flow results presented in Table 4.1.

Table 4.1. Load Flow results for inclusion of PMSG

BUS TYPE	VOLTAGE (in p.u)	P_G (in p.u)	Q_G (in p.u)	$-P_L$ (in p.u)	$-Q_L$(in p.u)
Swing	1.040∠0.000	1.5403	0.2264	-	-
P-V	1.025∠0.0007	1.6300	0.0245	-	-
P-Q	1.039∠0.0025	-	-	0.0158	0
P-Q	1.031∠-0.0014	-	-	0	0
P-Q	1.0028∠-0.0024	-	-	1.25	0.5
P-Q	1.0202∠-0.0027	-	-	0.9	0.3
P-Q	1.0280∠-0.0010	-	-	0	0
P-Q	1.0193∠-0.0023	-	-	1	0.35
P-Q	1.039∠-0.0025	-	-	0	0

Table 4.2. Eigenvalues for inclusion of PMSG

MODES	EIGEN VALUES	OSCILLATION FREQUENCY	DAMPING RATIO
δ_3	0	0	0
δ_2, ω_2	-7.3571 +/- 52.5151i	8.3580	0.1387
δ_1, ω_1	-1.2196 +/- 17.6519i	2.8094	0.0689
V_{dc}, X_V	-2.6256 +/- 6.5253i	1.0385	0.3733
E_{d2}, X_4	-5.6816 +/ 3.1660i	0.5039	0.8735
E_{fd1}	-4.7928	0.4689	1.0000
E_{fd2}	-4.9511	0	1.0000
E_{q1}	-0.0510	0	1.0000
E_{q2}	-0.2995	0	1.0000
ω_3, X_W	-17.2717 +/- 5.9178i	0.9418	0.9460
E_{d1}	-3.2258	0	1.0000

The system remains stable after suffering a small disturbance since all eigenvalues have negative real parts. Five complex conjugate eigen values represent the four oscillatory modes. The six negative real eigenvalues represent the three non-oscillatory modes.

Table 4.3.Participation Factor for inclusion of PMSG

0	0.2452	0.2452	0.2646	0.2646	0	0	0.0004	0.0004	0.0002	0	0	0	0	0	0
0	0.2451	0.2451	0.2644	0.2644	0	0	0.0004	0.0004	0.0002	0	0	0	0	0	0
0	0.0007	0.0007	0.0013	0.0013	0	0	0.0479	0.0479	0.0554	0.0007	1.0813	0.0445	0	0	0
0	0	0	0	0	0	0	0	0	0	0	0	0	0	0	1
0	0	0	0.0002	0.0002	0	0	0.0625	0.0625	1.2847	0.0724	0.1206	0.0011	0	0	0
0	0.2732	0.2732	0.2558	0.2558	0	0	0.0185	0.0185	0.0004	0.0047	0	0.0018	0	0	0
0	0.2727	0.2727	0.2553	0.2553	0	0	0.0166	0.0166	0.0004	0.004	0.0001	0.0028	0	0	0
0	0.0615	0.0615	0.0142	0.0142	0	0	0.0277	0.0277	0.0019	0.01	0.0535	0.8924	0	0	0
0	0.075	0.075	0.0431	0.0431	0.0001	0.0001	0.5512	0.5512	0.0141	0.0462	0.0002	0.054	0	0	0
0	0.0002	0.0002	0.0001	0.0001	0	0	0.0163	0.0163	0.0417	1.0078	0.0018	0.011	0	0	0
0	0	0	0	0	0	0	0	0	0	0	0	0	1.5426	1.5426	0
1	0	0	0	0	0	0	0	0	0	0	0	0	0	0	0
0	0	0	0	0	0.5391	0.5391	0.0002	0.0002	0	0	0	0	0	0	0
0	0	0	0	0	0	0	0	0	0	0	0	0	1.5426	1.5426	0
0	0	0	0	0	0.5392	0.5392	0.0003	0.0003	0	0	0	0	0	0	0
0	0.0021	0.0021	0.0013	0.0013	0.0003	0.0003	0.6402	0.6402	0.2041	0.0365	0.0123	0.004	0	0	0

Table 4.4 Effect of wind variation (For 5 m/s and 11.5 m/s)

0	0.2452	0.2452	0.2646	0.2646	0	0	0.0004	0.0004	0.0002	0	0	0	0	0	0
0	0.2451	0.2451	0.2644	0.2644	0	0	0.0004	0.0004	0.0002	0	0	0	0	0	0
0	0.0007	0.0007	0.0013	0.0013	0	0	0.0479	0.0479	0.0554	0.0007	1.0813	0.0445	0	0	0
0	0	0	0	0	0	0	0	0	0	0	0	0	0	0	1
0	0	0	0.0002	0.0002	0	0	0.0625	0.0625	1.2847	0.0724	0.1206	0.0011	0	0	0
0	0.2732	0.2732	0.2558	0.2558	0	0	0.0185	0.0185	0.0004	0.0047	0	0.0018	0	0	0
0	0.2727	0.2727	0.2553	0.2553	0	0	0.0166	0.0166	0.0004	0.004	0.0001	0.0028	0	0	0
0	0.0615	0.0615	0.0142	0.0142	0	0	0.0277	0.0277	0.0019	0.01	0.0535	0.8924	0	0	0
0	0.075	0.075	0.0431	0.0431	0.0001	0.0001	0.5512	0.5512	0.0141	0.0462	0.0002	0.054	0	0	0
0	0.0002	0.0002	0.0001	0.0001	0	0	0.0163	0.0163	0.0417	1.0078	0.0018	0.011	0	0	0
0	0	0	0	0	0	0	0	0	0	0	0	0	1.5426	1.5426	0
1	0	0	0	0	0	0	0	0	0	0	0	0	0	0	0
0	0	0	0	0	0.5391	0.5391	0.0002	0.0002	0	0	0	0	0	0	0
0	0	0	0	0	0	0	0	0	0	0	0	0	1.5426	1.5426	0
0	0	0	0	0	0.5392	0.5392	0.0003	0.0003	0	0	0	0	0	0	0
0	0.0021	0.0021	0.0013	0.0013	0.0003	0.0003	0.6402	0.6402	0.2041	0.0365	0.0123	0.004	0	0	0

A. INFERENCE FROM PARTICIPATION FACTOR MATRIX

The participation factor gives the role played by a state variable in a particular mode. It is measure of relative participation of a state variable.

Table 4.4 represents the Eigen values of PMSG with the effect of wind variation 5 m/s,11.5 m/s. The small signal stability analysis is performed for possible minimum (5 m/s) and maximum wind speed (11.5 m/s).The result shows that the damping ratio of mechanical mode SG 1 reduced by 11%. The damping ratio of electrical mode of PMSG increases by 53.8%.

Table 4.5. Load Flow results for inclusion of PMSG and Induction generator

BUS TYPE	VOLTAGE (in p.u)	P_G (in p.u)	Q_G (in p.u)	$-P_L$ (in p.u)	$-Q_L$ (in p.u)
Swing	1.040∠0.000	1.5403	0.2264	-	-
P-V	1.025∠0.0396	1.6300	0.0306	-	-
P-Q	1.0388∠-0.141	-	-	0.0158	0
P-Q	1.0308∠-0.0824	-	-	0	0.05
P-Q	1.0027∠-0.1393	-	-	1.25	0.5
P-Q	1.0201∠-0.1538	-	-	0.9	0.3
P-Q	1.0280∠-0.0572	-	-	0	0
P-Q	1.0193∠-0.1319	-	-	1	0.35
P-Q	1.0388∠-0.1419	-	-	0	0

Table 4.6. Eigenvalues for inclusion of PMSG and Induction generator

MODES	EIGEN VALUES	OSCILLATION FREQUENCY	DAMPING RATIO
δ_4	0	0	0
ω_2, E_m	-10.8513 +/- 8.330i	1.3259	0.6292
δ_1, ω_1	-0.5891 +/- 8.2051i	1.3059	0.0051
E_c	-9.5838	0	1.0000
V_{dc} ,X_V	-2.6262 +/- 6.5251i	1.0385	0.1394
X_4,E_{fd1},E_{fd2}	-3.2269 +/- 2.9459i	0.4689	0.5454
X_4,E_{d1},E_{d2}	-3.6426	0	1.0000
E_{fd1},E_{q1}	-3.0898 +/- 1.4465i	0.2302	0.8202
E_{q2}	-1.4786	0	1.0000
δ_1, δ_2	-0.0000	0	1.0000
$\delta_1, \omega_1, \delta_2, \omega_2$	-0.3474	0	1.0000
ω_4, X_W	-17.2717 +/- 5.917i	0.9418	0.8949
E_{d1}	-3.2258	0	1.0000

B.INFERENCE FROM EIGENVALUES

The system remains stable after suffering a small disturbance since all eigenvalues have negative real parts.Six complex conjugate eigen values represent the four oscillatory modes. The six negative real eigenvalues represent the three non-oscillatory modes.

Table 4.7.Participation Factor for inclusion of PMSG and Induction generator

0	0.0005	0.0005	0.1059	0.1059	0	0.0001	0.0001	0.0029	0.0029	0.0067	0.0036	0.0036	0.0017	0	0.7891	0	0	0
0	0.0005	0.0005	0.1057	0.1057	0	0.0001	0.0001	0.0028	0.0028	0.0063	0.0034	0.0034	0.0015	0.4812	0.3087	0	0	0
0	0	0	0.0004	0.0004	0.0003	0	0	0.236	0.236	0.1648	0.7113	0.7113	0.0179	0	0	0	0	0
0	0	0	0	0	0	0	0	0	0	0	0	0	0	0	0	0	0	1
0	0	0	0.0003	0.0003	0.0006	0	0	0.2939	0.2939	0.4176	0.9677	0.9677	0.0065	0	0	0	0	0
0	0.0003	0.0003	0.3964	0.3964	0	0.0001	0.0001	0.0125	0.0125	0.0346	0.0172	0.0172	0.0152	0	0.2125	0	0	0
0	0.0003	0.0003	0.3954	0.3954	0	0.0001	0.0001	0.0109	0.0109	0.0272	0.0137	0.0137	0.0072	0.4746	0.2653	0	0	0
0	0	0	0.0124	0.0124	0.0001	0	0	0.2835	0.2835	0.0622	0.2239	0.2239	0.847	0	0.0002	0	0	0
0	0	0	0.0166	0.0166	0.0005	0.0001	0.0001	0.0915	0.0915	0.6512	0.1787	0.1787	0.2675	0	0	0	0	0
0	0	0	0.0042	0.0042	0.0001	0	0	0.3473	0.3473	0.1659	0.3114	0.3114	0.3238	0	0	0	0	0
0	0.485	0.485	0	0	0.0342	0	0	0	0	0	0	0	0	0	0.0005	0	0	0
0	0.0205	0.0205	0	0	0.9684	0	0	0.0009	0.0009	0	0.0003	0.0003	0	0.0014	0.0015	0	0	0
0	0.5063	0.5063	0	0	0.0039	0	0	0	0	0.0001	0	0	0	0.0456	0.0471	0	0	0
0	0	0	0	0	0	0	0	0	0	0	0	0	0	0	0	1.5426	1.5426	0
1	0	0	0	0	0	0	0	0	0	0	0	0	0	0	0	0	0	0
0	0	0	0	0	0	0.539	0.539	0.0002	0.0002	0	0	0	0	0	0	0	0	0
0	0	0	0	0	0	0	0	0	0	0	0	0	0	0	0	1.5426	1.5426	0
0	0	0	0	0	0	0.5391	0.5391	0.0002	0.0002	0	0	0	0	0	0	0	0	0
0	0	0	0.0006	0.0006	0.0004	0.0004	0.0004	0.2571	0.2571	0.5726	0.2328	0.2328	0.2234	0	0	0	0	0

The participation matrix gives the role of state variables in particular modes. The state variables that influences the modes are shown in table 4.5.

C.OPTIMISED VALUES

For the above cases the values of controller parameters are chosen by trial and error method. Thus the values are optimized using genetic algorithm technique and eigenvalues are tabulated.

Tuned Parameters values for inclusion of PMSG

K_{pw}=11.3112 p.u T_w=0.4941sec

K_{pv}=8.2219 p.u T_v=0.1641sec

K_{p1}=2.8264 p.u T_4=0.1587 sec

Table 4.8. Improved Eigenvalues for inclusion of PMSG

NO	EIGEN VALUES (*e0.02)	OSCILLATION FREQUENCY	DAMPING RATIO
1	0	0	0
2	-0.7506	0	1
3,4	-0.0738 +/- 0.5281i	8.4050	0.1384
5,6	-0.0124 +/- 0.1765i	2.81	0.0701
7,8	-0.0555 +/- 0.0397i	6.3	0.8133
9	-0.0661	0	1
10	-0.0473	0	1
11	-0.0496	0	1
12	-0.0005	0	1
13	-0.0030	0	1
14	-7.5328	0	1
15	-0.0201	0	1
16	-0.0323	0	1

Table 4.9. Improved Eigenvalues for inclusion of PMSG and Induction generator

NO	EIGEN VALUES (*e0.02)	OSCILLATION FREQUENCY	DAMPING RATIO
1	0	0	0
2	-0.6913	0	1
3,4	-0.1085 +/- 0.0833i	1.33	0.7932
5,6	-0.0059 +/- 0.0820i	1.31	0.0718
7	-0.0959	0	1
8	-0.0688	0	1
9,10	-0.0267 +/- 0.0290i	0.46	0.6773
11,12	-0.0346 +/-0.0131i	0.21	0.9352
13	-0.0000	0	1
14	-0.0035	0	1
15	-0.0100	0	1
16	-0.0236	0	1
17	-7.0080	0	1
18	-0.0279	0	1
19	-0.0323	0	1

Tuned values for inclusion of PMSG and induction generator

K_{pw}= 10.5359 p.u T_w= 0.3592 sec

K_{pv}=7.6496 p.u T_v=0.1591 sec

K_{p1}= 1.8919 p.u T_4= 0.2298 sec

IV. CONCLUSION

TTBS with and without DSSC are simulated. The results indicate that the voltage, real power and reactive power are improved by the addition of DSSC. The increase in V,P and Q are due to increase in voltage with the addition of DSSC. DSSC has the ability to compensate the voltage sag in power and distribution lines. The disadvantage of DSSC is that the hardware cost is increased.

The present work deals with TTBS with and without DSSC. Studies on closed loop TTBS with PI and PR systems will be done in future.

REFERENCES

[1] Sharma, R.K., Irusapparajan, G. & Periyaazhagar, D. 2019, "Three-phase symmetric cascading Z-source seven levels multilevel inverter excited by multi carrier sinusoidal pulse width modulation scheme", International Journal of Innovative Technology and Exploring Engineering, vol. 8, no. 10, pp. 4269-4274.

[2] Velavan, R., Bharanidharan, S. & Sheeba, B. 2019, "EMF pollution - Causes, effects and protection", International Journal of Innovative Technology and Exploring Engineering, vol. 8, no. 9 Special Issue 3, pp. 1166-1168.

[3] Saravana, S., Balaji, S., Arulselvi, S. & John Paul Praveen, A. 2019, "Reliable power quality monitoring and protection system", International Journal of Innovative Technology and Exploring Engineering, vol. 8, no. 9 Special Issue 3, pp. 644-645.

[4] Tamil Selvan, S. & Sundararajan, M. 2019, "Performance Parameters of 3 Value 8t Cntfet Based Sram Cell Design Using H-Spice", International Journal of Recent Technology and Engineering, vol. 8, no. 2 Special issue 5, pp. 22-27.

[5] Jac Fredo, A.R., Abilash, R.S., Femi, R., Mythili, A. & Kumar, C.S. 2019, "Classification of damages in composite images using Zernike moments and support vector machines", Composites Part B: Engineering, vol. 168, pp. 77-86.

[6] Kathiravan, P. & Govindaraju, C. 2019, "Design and evaluation of ultra gain isolated DC-DC converter for photovoltaic system", International Journal of Engineering and Advanced Technology, vol. 8, no. 5, pp. 2646-2651.

[7] Kripa, N., Vasuki, R. & Kishore Kanna, R. 2019, "Realtime neural interface controlled au-pair BIMA bot", International Journal of Recent Technology and Engineering, vol. 8, no. 1, pp. 992-994.

[8] Mohanraj, Meenaa Kumari, M., Philomina, S. & Jasmin, M. 2019, "In-situ humidity measurement of hydrogen fuel cell car using MEMS sensor", International Journal of Recent Technology and Engineering, vol. 8, no. 1, pp. 41-43.

[9] Velmurugan, T. & Prakash, S. 2019, "Artificial intelligent based distribution automation of swift fault detection isolation and power restoration for HT network", International Journal of Innovative Technology and Exploring Engineering, vol. 8, no. 6, pp. 1-6.

[10] Dwarakesh, K. & Prem Kumar, G. 2019, "Five-level inverter based sequential boost system using fuzzy logic controller", International Journal of Innovative Technology and Exploring Engineering, vol. 8, no. 6, pp. 12-19.

[11] Anne Gifta, A. & Hemavathi, G. 2019, "Analysis of grid tied solar PV system using ANFIS Algorithm", International Journal of Innovative Technology and Exploring Engineering, vol. 8, no. 6, pp. 312-316.

[12] Jayavel, R., Rangaswamy, T.R. & Prakash, S. 2019, "Efficient grid management system with renewable and conventional power sources", International Journal of Innovative Technology and Exploring Engineering, vol. 8, no. 6, pp. 287-289.

[13] Hemavathi, G. & Maheshwaran, S. 2019, "Proportional resonant controlled high gain step-up converter system with improved response", International Journal of Innovative Technology and Exploring Engineering, vol. 8, no. 6, pp. 317-323.

[14] Periyaazhagar, D. & Irusapparajan, G. 2019, "Design and completion of asymmetric single phase 27 level cascaded mli for various pwm scheme", International Journal of Innovative Technology and Exploring Engineering, vol. 8, no. 6, pp. 792-797.

[15] Mahalakshmi, V. & Vijayaragavan, S.P. 2019, "PV based power electronic converters for high voltage DC applications", International Journal of Recent Technology and Engineering, vol. 7, no. 6, pp. 670-674.

[16] Irusapparajan, G., Periyaazhagar, D., Prabaharan, N. & Rini Ann Jerin, A. 2019, "Experimental verification of trinary DC source cascaded h-bridge multilevel inverter using unipolar pulse width modulation", Automatika, vol. 60, no. 1, pp. 19-27.

[17] Sangeetha, G., Sherine, S., Arputharaju, K. & Prakash, S. 2019, "On Line Monitoring of Higher Rated Alternator using Automated Generator Capability Curve Administer", Proceedings of the IEEE International Conference on "Recent Trends in Electrical, Control and Communication", RTECC 2018, pp. 176.

[18] Bycil, V.J. & Wiselin, M.C.J. 2019, "Modeling and analysis of vibration energy harvesting system using piezo stack", International Journal of Mechanical and Production Engineering Research and Development, vol. 9, no. Special Issue 1, pp. 523-533.

[19] Sripada, A., Warrier, A., Kapoor, A., Gaur, H. & Hemalatha, B. 2018, "Dynamic lateral balance of humanoid robots on unstable surfaces", International Conference on Electrical, Electronics, Communication Computer Technologies and Optimization Techniques, ICEECCOT 2017, pp. 539.

[20] Srinivasan, S., Thirumalaivasan, K. & Sivakumaran, T.S. 2018, "Performance evaluation of double-output luo converters", Journal of Advanced Research in Dynamical and Control Systems, vol. 10, no. 10 Special Issue, pp. 870-878.

[21] Karthikayen, A. & Selvakumar Raja, S. 2018, "A skellam distribution inspired trust factor-based selfish node detection technique in MANETs", Journal of Advanced Research in Dynamical and Control Systems, vol. 10, no. 13, pp. 940-949.

AUTHORS PROFILE

S.Aarthi Suriya, Assistant Professor Department of EEE, Bharath Institute of Higher Education and Research, Tamilnadu, India.

Anitha SampathKumar, Assistant Professor ,Department of EEE, Bharath Institute of Higher Education and Research, Tamilnadu, India.

S.Sherine Assistant Professor Department of EEE, Bharath Institute of Higher Education and Research, Tamilnadu, India.